Information-Theoretic Sensor and Excitation Design for Observable Multiphase Two-Fluid Networks with Entropy Constraints

Hendra Wijaya[1] **and Bagus Firmansyah**[2]

[1]Universitas Negeri Gorontalo, Faculty of Engineering, Department of Informatics Engineering, Jalan Jenderal Sudirman No. 6, Dulalowo Timur, Kota Tengah, Gorontalo, Indonesia

[2]Universitas Lambung Mangkurat, Faculty of Engineering, Department of Information Technology, Jalan A. Yani KM 36, Banjarbaru, South Kalimantan, Indonesia

ABSTRACT Multiphase thermal-hydraulic networks are monitored and controlled through sparse, heterogeneous sensors whose placement is often determined by convenience rather than identifiability. In gas–liquid systems, macroscopic predictions depend on partially observed internal states and on regime-dependent transport mechanisms that change with operating point and geometry. This paper develops a principled framework for joint sensor placement and input excitation design in networked two-fluid models, targeting state and parameter observability under thermodynamic admissibility constraints. The core idea is to quantify the value of a sensing configuration by its expected information gain about latent flow structure, computed from a constrained probabilistic dynamics model whose evolution operator is entropy stable and positivity preserving. Design variables include discrete sensor locations, sensor modalities with distinct noise and bandwidth properties, and admissible actuation trajectories that excite informative modes without violating safety limits. The resulting problem is posed as a mixed discrete–continuous optimization over mutual information and D-optimality surrogates derived from trajectory-dependent sensitivity operators. To make the design tractable at network scale, the approach introduces amortized adjoint computations for entropy-stable semidiscretizations, and it employs relaxation-based approximations for Fisher information that remain accurate in stiff, regime-transitioning conditions. Computational studies in annular and branched configurations demonstrate that optimal designs shift instrumentation toward junction-adjacent segments and prioritize differential measurements that condition latent slip and holdup modes, while carefully shaped boundary excitations can reduce posterior uncertainty without increasing risk. The framework provides a technical basis for instrumentation decisions in multiphase systems where sensing is expensive and observability is inherently limited.

1. Introduction

Instrumentation in multiphase thermal-hydraulic systems is frequently treated as an engineering afterthought, yet it is a first-order determinant of what can be inferred, controlled, and certified. In gas–liquid networks, the internal state that drives safety constraints and performance objectives is distributed in space, strongly nonlinear, and only partially observed through signals such as pressures, differential pressures, point temperatures, and occasionally integrated void fraction proxies. Even when a mechanistic two-fluid model is available, its predictive utility hinges on how well the unmeasured state can be reconstructed and how much of the latent interfacial structure can be constrained by the available sensors. When observability is poor, the same measured pressures can be explained by multiple internal configurations that differ substantially in void fraction distribution, slip, and phase momentum partitioning. This ambiguity propagates into conservative operating margins, delayed fault

Article info:
Hendra Wijaya and Bagus Firmansyah. *Information-Theoretic Sensor and Excitation Design for Observable Multiphase Two-Fluid Networks with Entropy Constraints.* Center for Theoretical and Applied STEM Research (CTASR) . Licensed under Attribution - NonCommercial - No Derivatives 4.0 International (CC BY-NC-ND 4.0)

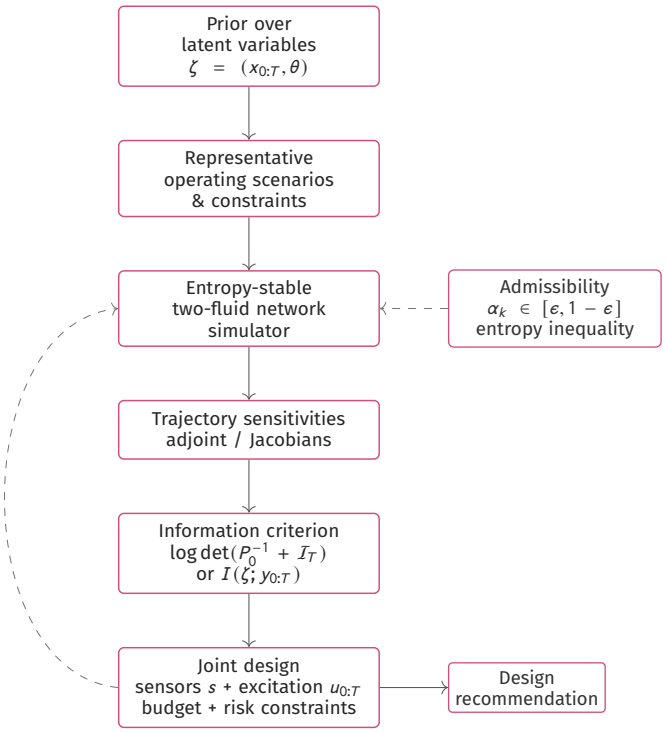


Figure 1 End-to-end design loop: admissible two-fluid network simulation feeds trajectory sensitivities and information metrics, enabling joint optimization of sparse heterogeneous sensing and safe excitation trajectories over representative scenarios.

detection, and brittle control actions that rely on unverified internal estimates.

The practical difficulty is not merely that sensors are sparse, but that multiphase dynamics are structurally ill-conditioned for inference. The mapping from state to measurements is often low rank because many sensors integrate information over a long segment and are primarily sensitive to aggregate pressure loss rather than local holdup. The dynamics can also dissipate high-frequency perturbations rapidly, meaning that even if a local disturbance is present, it may not leave a persistent signature in boundary measurements [1]. In addition, the effective transport mechanisms change with operating conditions: a small change in inlet quality or backpressure can reorganize interfacial structure and alter slip, friction partitioning, and heat transfer, which in turn changes the sensitivity of measured signals to internal variables. Under these conditions, naive sensor placement rules, such as uniformly spaced pressure taps or only inlet/outlet instrumentation, can leave the system practically unobservable in precisely those regimes where inference is most needed.

Data-driven regime recognition results underscore that measurable signals can contain rich information about multiphase structure even when mechanistic state is not directly observed. Manikonda et al. (2021) reported an early and unusually high-performing set of machine-learning classifiers that could infer gas–liquid flow regimes in annular-channel settings with near real-time latency and accuracy close to 98%, indicating that regime-dependent interfacial configurations can be detected reliably from accessible features [2]. That capability is relevant here not because regime labels are the target of this paper, but because it motivates an information-theoretic view: if measurements contain latent structure information, then the question becomes which measurements, at which locations, and under which excitations make that information identifiable for the variables that matter for prediction and safety.

This paper develops a framework for designing instrumentation and excitation to maximize observability in networked two-fluid models while respecting thermodynamic admissibility. The design objective is not to fit a closure model or to construct a surrogate, but to select a measurement architecture that yields posterior contraction on latent state variables and critical uncertain quantities under a constrained probabilistic dynamics model [3]. The central thesis is that the value of a sensor configuration must be evaluated on trajectories, not at a single operating point, because sensitivity and information content are transient and regime dependent. Furthermore, the design must account for physical constraints that exclude many mathematically optimal excitations; the most informative boundary perturbation may be unsafe, and a physically consistent design must balance identifiability against risk.

The approach is built on four ingredients that are combined into a single optimization formulation. The first ingredient is a networked two-fluid semidiscretization that is entropy stable and positivity preserving, so that

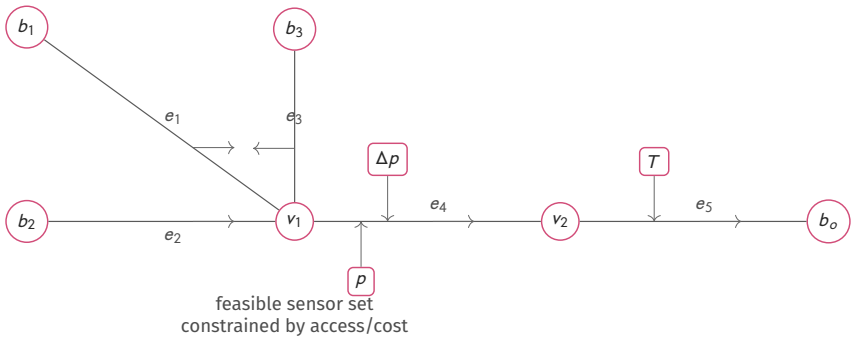


Figure 2 Directed-graph abstraction of a multiphase network: edges are conduit segments and nodes are junction/boundary manifolds. Candidate sensing is represented as localized modalities (e.g., p, Δp, T) placed near junction-adjacent segments that frequently dominate identifiability.

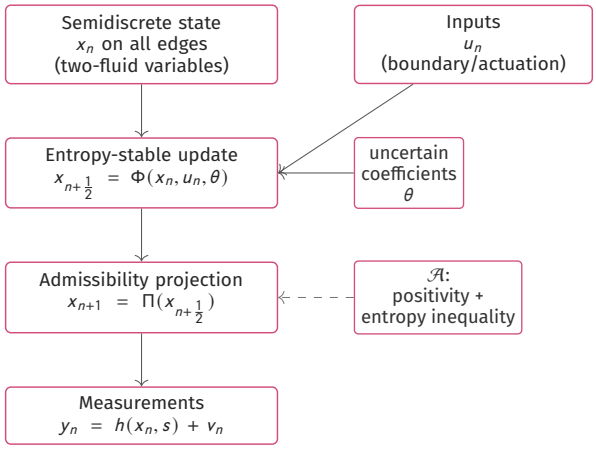


Figure 3 Entropy-stable time stepping with an admissibility projection: the update evolves the two-fluid network state and then enforces positivity and a discrete entropy inequality before producing sensor predictions through a modality- and placement-dependent measurement map.

sensitivity analysis and information measures are computed on admissible trajectories rather than on unphysical states. The second ingredient is a probabilistic model of process noise, sensor noise, and model discrepancy that yields a coherent posterior distribution, so that information gain can be defined as a reduction in posterior uncertainty rather than as an ad hoc sensitivity metric. The third ingredient is an information criterion, based on mutual information and D-optimality surrogates, that quantifies how a candidate sensing architecture constrains latent variables of interest along representative trajectories. The fourth ingredient is a computational strategy that makes the resulting mixed discrete–continuous optimization feasible: adjoint-based gradient evaluation for continuous excitation variables, relaxations and greedy selection for discrete sensor placement, and amortization of sensitivity computations across candidate architectures.

The contribution differs from classical optimal experimental design in fluid systems in two ways [4]. First, it emphasizes admissibility and entropy consistency as constraints that shape sensitivity and information. In multiphase models, sensitivity computed about unphysical or entropy-violating trajectories can be misleading because it may exaggerate unstable modes that are artifacts of an inadmissible closure or discretization. Second, it targets networked systems where junction coupling and boundary interactions dominate observability, so that optimal instrumentation is not a simple extension of single-pipe sensor placement. The framework explicitly accounts for graph topology and for the fact that junction regions can act as information bottlenecks in which local uncertainty propagates nonlinearly into downstream measurements.

The paper is organized to reflect the logic of the design problem. The next section formalizes the networked two-fluid model, the admissibility constraints, and a measurement abstraction that captures sensor heterogeneity and time aggregation. The third section develops trajectory-dependent information measures, including mutual information approximations and Fisher information operators, and relates them to observability in nonlinear dissipative systems. The fourth section formulates the joint sensor and excitation design as a constrained mixed optimization problem and derives computationally tractable relaxations, including adjoint-based gradients under entropy-stable updates and greedy selec-

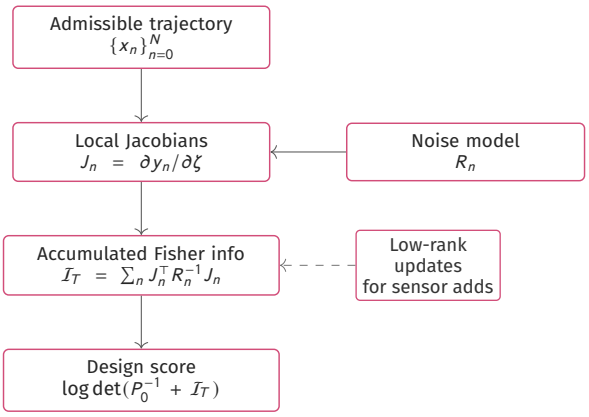


Figure 4 Trajectory-dependent information evaluation: local sensitivities and sensor-noise models accumulate into a Fisher-information operator that supports D-optimal surrogates for expected information gain and efficient low-rank updates during sensor selection.

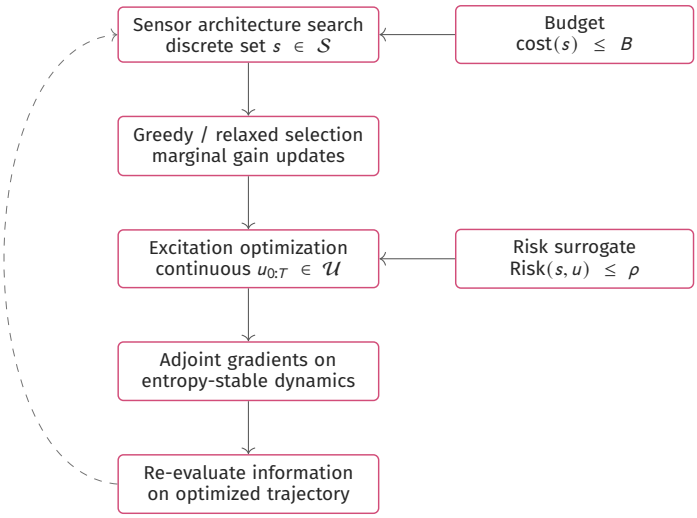


Figure 5 Mixed discrete–continuous design strategy: sensor placement is updated via marginal information gain under budget limits, while admissible boundary excitations are refined by adjoint gradients under explicit risk constraints to maximize trajectory information content.

tion criteria with submodular structure under suitable approximations [5]. The final section presents computational studies in annular and branched configurations that illustrate how the optimal design reallocates sensors and prescribes safe excitations that improve identifiability, and it discusses failure modes where observability is fundamentally limited. The conclusion summarizes implications for instrumentation practice in multiphase thermal-hydraulic networks.

2. Networked Two-Fluid Dynamics, Admissibility, and Measurement Abstractions

Consider a directed graph representation of a multiphase network in which each edge corresponds to a conduit segment and each node corresponds to a junction or boundary manifold. On each edge, cross-sectionally averaged two-fluid balance laws evolve phase masses, phase momenta, and phase energies. Let $k \in \{g, \ell\}$ denote gas and liquid. With volume fractions $\alpha_k(x,t)$ satisfying $\alpha_g + \alpha_\ell = 1$, phase densities ρ_k, velocities u_k, and specific total energies $E_k = e_k + \frac{1}{2}u_k^2$, define conservative variables per edge cell. The evolution on an edge is written in semidiscrete form as

$$\begin{aligned} \dot{x}(t) &= f\big(x(t), u(t), \theta\big) \quad + \quad w(t) \\ y(t) &= h\big(x(t), s\big) \quad + \quad v(t), \end{aligned} \tag{1}$$

where $x(t) \in \mathbb{R}^{n_x}$ stacks all edge cell conservative variables and selected node variables, $u(t) \in \mathbb{R}^{n_u}$ represents boundary and actuation inputs, and $\theta \in \mathbb{R}^{n_\theta}$ collects uncertain but slowly varying coefficients such as effective friction scalings, junction loss scalings, or heat transfer multipliers. The process noise $w(t)$ represents unresolved turbulence, unmodeled small-scale variability, and discretization error, while the measurement noise $v(t)$ represents sensor noise and telemetry imperfec-

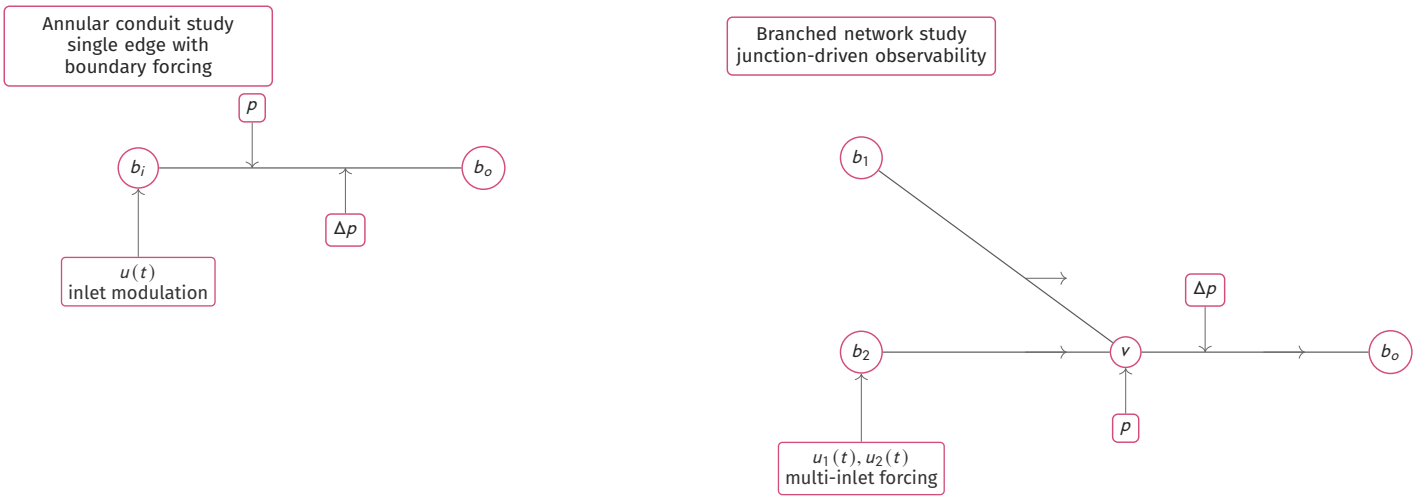


Figure 6 Study configurations used to evaluate design outcomes: a single annular conduit highlights differential measurements under shaped boundary forcing, while a branched network emphasizes junction-adjacent sensing that breaks confounding between branch losses and junction coupling.

tions. The sensor architecture is represented by a discrete design variable s encoding which sensors are deployed, where they are placed, and which modality each sensor implements.

The dynamics function f is induced by an entropy-stable spatial discretization on each edge coupled through junction constraints at nodes [6]. The junction coupling enforces conservation while allowing pressure losses and phase split behavior. For a node v with incident edges $\mathcal{E}(v)$, a representative conservation condition is

$$\sum_{e \in \mathcal{E}(v)} s_{ve} \, F_{e,k}(x, u, \theta) \;=\; 0, \tag{2}$$

where $F_{e,k}$ denotes the phase mass flux and s_{ve} encodes the edge orientation relative to the node. Similar conditions apply to total enthalpy flux. In practice, junction models include additional algebraic constraints for pressure and split fractions that can be nondifferentiable if implemented with case logic. The present framework assumes a differentiable junction representation, either by smoothing switching relations or by using continuously parameterized split functions, because sensitivity and information computation require differentiability along trajectories.

Admissibility is imposed through an entropy inequality and positivity conditions. Let $\eta(x)$ denote a convex entropy functional for the semidiscrete two-fluid system and let $\psi(x)$ denote its associated entropy flux. Entropy stability at the discrete level is enforced by requiring that, for each time step, the update satisfies a discrete inequality of the form

$$\begin{aligned} \eta(x_{n+1}) - \eta(x_n) &\le \Delta t \, \Sigma(x_n, u_n, \theta) \\ \Sigma(x_n, u_n, \theta) &\le 0, \end{aligned} \tag{3}$$

where Σ represents dissipative entropy production contributions. Alongside entropy, positivity constraints enforce $\alpha_k \in [\epsilon, 1-\epsilon]$ and nonnegativity of phase masses and internal energies within bounds compatible with the equation of state [7]. The role of these constraints in instrumentation design is subtle but important. Sensitivity and information computed about inadmissible trajectories can artificially inflate certain unstable modes and bias placement toward sensors that are only informative for unphysical behaviors. By computing information on admissible trajectories, the design aligns with physically realizable dynamics and avoids pathological solutions that would vanish under a physically consistent solver.

The measurement operator $h(x, s)$ encapsulates sensor selection and placement. Each sensor is defined by a modality and a location, and many modalities are naturally expressed as linear or weakly nonlinear functionals of the state. A point pressure sensor is modeled as a mapping to the local pressure variable computed from conservative variables and the equation of state, while a differential pressure sensor is modeled as a difference of pressures at two locations. A temperature sensor is similarly modeled as a local temperature computed from phase energies and compositions. Time aggregation is incorporated by allowing each sensor to report a filtered value over a window, which is common for flow meters and for telemetry that transmits averages [8]. A generic aggregated measurement at time t_n is

$$y_n = \frac{1}{\Delta} \int_{t_n - \Delta}^{t_n} h\big(x(t), s\big) \, dt \quad + \quad v_n, \tag{4}$$

which can be embedded into the state-space model by augmenting the state with filter memory or by approximating the integral with quadrature along the predicted trajectory.

The sensor design variable s is discrete and combina-

Table 1 Elements of the networked two-fluid state-space representation.

Symbol	Description	Notes
$x(t) \in \mathbb{R}^{n_x}$	Stacked conservative variables on edges and selected node variables	Includes phase masses, momenta, and energies for gas and liquid on each edge cell
$u(t) \in \mathbb{R}^{n_u}$	Boundary and actuation inputs	Inlet mass flows, valve positions, pump speeds, imposed heat fluxes
$\theta \in \mathbb{R}^{n_\theta}$	Slowly varying uncertain coefficients	Effective friction factors, junction loss scalings, heat transfer multipliers
$w(t)$	Process noise on dynamics	Represents unresolved turbulence, small-scale variability, discretization error
$v(t)$	Measurement noise	Accounts for sensor noise, telemetry imperfections, and time-aggregation effects
s	Discrete sensor architecture variable	Encodes locations, modalities, and feasibility constraints for deployed sensors

torial. It may encode whether a pressure tap is placed at a candidate cell, whether a differential pressure transducer spans a candidate segment, whether a temperature sensor is present at a node, and whether a holdup proxy is installed on an edge. Each deployed sensor has a cost, and the design must respect a budget. The design also must respect physical constraints: certain locations may be infeasible due to packaging, certain modalities may be excluded by safety regulations, and certain lines may be inaccessible. These constraints are represented by restricting the feasible set of s.

The excitation design variable is continuous [9]. It includes admissible boundary variations such as controlled inlet mass flow modulation, valve position variations, pump speed profiles, and heat flux modulation where applicable. Excitations must respect safety constraints on pressures and temperatures and must respect actuator bandwidth limits. A crucial feature of multiphase networks is that excitations can provoke regime transitions, which may increase information but also increase risk. The design must therefore include a risk-aware constraint on excitations, expressed in terms of predicted state envelopes or probabilistic safety margins under process noise.

Although this paper does not depend on regime classification models, it is useful to recognize that regime-dependent behavior can be detectable from practical measurements in annular geometries. Manikonda et al. (2022) extended the annular-channel regime prediction line by presenting highly accurate machine-learning classification models that infer gas–liquid flow regimes from measured features with state-of-the-art accuracy, reinforcing that measurable signals can discriminate interfacial configurations that drive closure changes [10]. In the present context, that observation motivates sensor design objectives that emphasize not only mean pressure-drop sensitivity but also sensitivity to latent slip and holdup modes that distinguish regime-dependent transport [11].

The design framework treats the dynamics model as a probabilistic mapping from inputs to measurements. For a given design $(s, u_{0:T})$ over a horizon T, one can define the joint distribution of latent variables and measurements. Let ζ denote the latent quantities of interest for inference, which may include a subset of the state trajectory, a reduced representation of internal holdup fields, and uncertain coefficients θ. The value of a design is then quantified as how much the measurements reduce uncertainty about ζ. This reduction is formalized in the next section through mutual information and Fisher information approximations that can be computed along admissible trajectories.

Table 2 Admissibility conditions in the entropy-stable networked two-fluid model.

Constraint type	Mathematical form	Role in design
Discrete entropy inequality	$\eta(x_{n+1}) - \eta(x_n) \leq \Delta t\, \Sigma(x_n, u_n, \theta)$, $\Sigma \leq 0$	Ensures entropy-stable evolution and suppresses spurious numerical instabilities
Positivity of phases	$\alpha_k \in [\epsilon, 1-\epsilon]$, nonnegative masses and internal energies	Prevents unphysical void fractions and negative energies in trajectory simulation
Equation-of-state consistency	Pressure and temperature derived from conservative variables	Couples phase fields to thermodynamic variables used in sensing and risk constraints
Junction conservation	$\sum_{e \in \mathcal{E}(v)} s_{ve} F_{e,k}(x, u, \theta) = 0$	Enforces mass and enthalpy conservation at nodes with differentiable split models
Safety envelope	$c(x(t)) \leq 0$ or probabilistic variants over $[0, T]$	Constrains pressures, temperatures, and holdup within acceptable operating limits

3. Trajectory-Dependent Information Measures for Observability

Observability in nonlinear dissipative systems is not a binary property but a spectrum that depends on operating conditions, sensor architecture, and excitation. For multiphase networks, the sensitivity of measurements to internal states can change abruptly when a regime transition shifts the effective coupling between phases. It is therefore natural to formulate instrumentation design in terms of information measures that explicitly depend on trajectories. This section develops such measures and explains their connection to posterior contraction for latent variables of interest [12].

Let ζ denote latent variables to be inferred, with prior density $p(\zeta)$. Given a design consisting of a sensor architecture s and an excitation input $u_{0:T}$, let $y_{0:T}$ denote the resulting measurement sequence with conditional density $p(y_{0:T} \mid \zeta, s, u_{0:T})$. The expected information gain about ζ is defined as the mutual information

$$I(\zeta;\, y_{0:T} \mid s, u_{0:T}) = \mathbb{E}\Big[\log \frac{p(y_{0:T} \mid \zeta, s, u_{0:T})}{p(y_{0:T} \mid s, u_{0:T})}\Big], \tag{5}$$

where the expectation is taken under the joint distribution induced by the prior and the likelihood. Maximizing this quantity over s and $u_{0:T}$ yields a design that, in expectation, most reduces posterior uncertainty. In practice, exact mutual information is difficult to compute for high-dimensional nonlinear models, and so tractable approximations are required.

A common approximation for information design is based on Gaussian linearization about a nominal trajectory. Suppose ζ parameterizes initial conditions and uncertain coefficients, and suppose the measurement map is differentiable. Linearizing the measurement prediction around a nominal $\bar{\zeta}$ yields

$$y \approx \hat{y}(\bar{\zeta}) \quad + \quad J(\bar{\zeta})\,(\zeta - \bar{\zeta}) \quad + \quad \epsilon, \tag{6}$$

where J is the Jacobian of the stacked measurement sequence with respect to ζ and ϵ represents aggregated noise. If the prior on ζ is Gaussian with covariance P_0 and the noise is Gaussian with covariance R, the posterior covariance is

$$P_{\text{post}}^{-1} = P_0^{-1} \quad + \quad J^{\top} R^{-1} J. \tag{7}$$

The matrix $J^{\top} R^{-1} J$ is a Fisher information approximation. Information gain can then be related to the log determinant ratio of prior and posterior covariances [13]. A D-optimality surrogate for expected information gain is

$$\mathcal{J}_D(s, u_{0:T}) = \log\det\!\big(P_0^{-1} + J^{\top} R^{-1} J\big), \tag{8}$$

up to constants independent of design. This surrogate is attractive because it reduces information design to computing the sensitivity Jacobian J along the trajectory induced by $(s, u_{0:T})$, and then solving an optimization problem over a scalar objective.

In multiphase networks, naive linearization can fail near regime transitions because the Jacobian can change rapidly and the noise can be state dependent. To address

Table 3 Representative measurement modalities and their abstractions.

Modality	Measurement operator $h(x, s)$	Characteristics
Absolute pressure tap	Local pressure derived from conservative variables	Sensitive to integrated pressure loss and boundary conditions
Differential pressure transducer	Pressure difference across two points or segments	Enhances sensitivity to friction, slip, and junction losses; cancels common-mode errors
Point temperature sensor	Local temperature from phase energies and composition	Probes energy balance and heat transfer behavior
Holdup or void-fraction proxy	Local or segment-averaged void fraction functional	Direct information on interfacial configuration and slip-related modes where available
Time-averaged signal	$\frac{1}{\Delta}\int_{t_n-\Delta}^{t_n} h(x(t), s)\, dt$	Represents sensor filtering and telemetry averaging, attenuating high-frequency content

this, the framework uses trajectory-dependent local information accumulation. Let y_n denote measurements at times t_n and let J_n denote the Jacobian of y_n with respect to ζ. The accumulated information over a window is

$$\mathcal{I}_T = \sum_{n=0}^{N} J_n^\top R_n^{-1} J_n, \tag{9}$$

where R_n may depend on predicted sensor signal amplitude and bandwidth. This accumulation naturally accounts for transients: when an excitation causes a sensitive response, the corresponding J_n contributes strongly to $\mathcal{I}_T$. When the system is quiescent, $\mathcal{I}_T$ grows slowly. The D-optimality surrogate becomes $\log\det(P_0^{-1} + \mathcal{I}_T)$, which is explicitly trajectory dependent.

The Jacobians J_n can be computed by sensitivity propagation or by adjoint methods [14]. For high-dimensional multiphase states, direct sensitivity propagation is expensive because it scales with the dimension of ζ. Adjoint methods are preferred when ζ is high dimensional but the number of measurement channels is moderate. Let $x(t)$ evolve according to the admissible dynamics and let the measurement prediction be $y_n = h(x(t_n), s)$. The sensitivity of y_n to parameters and initial conditions involves the state transition operator. An adjoint formulation expresses gradients of an objective with respect to ζ in terms of backward integration of an adjoint variable. Because the design objective involves the log determinant of an information matrix rather than a simple scalar measurement mismatch, the adjoint must be embedded in a matrix calculus. A practical approach is to compute directional derivatives by sampling probe vectors, which enables stochastic trace and log determinant estimation.

To make these statements concrete, consider ζ composed of uncertain coefficients θ and an initial state component x_0 [15]. For a discretized time horizon with step size Δt, the state update is

$$x_{n+1} = \Phi\big(x_n, u_n, \theta\big) \quad + \quad \omega_n, \tag{10}$$

with Φ representing the entropy-stable projected update. Define the linearized transition matrices

$$\begin{aligned} A_n &= \frac{\partial \Phi}{\partial x}(x_n, u_n, \theta), \\ B_n &= \frac{\partial \Phi}{\partial \theta}(x_n, u_n, \theta), \end{aligned} \tag{11}$$

and the measurement Jacobian

$$C_n = \frac{\partial h}{\partial x}(x_n, s). \tag{12}$$

Then the sensitivity of measurements to parameters can be expressed through a recursion for a sensitivity state, but in adjoint form, gradients can be computed by backward recursion. While the full derivation is lengthy, the key computational point is that the matrices A_n inherit stability from the entropy-stable projection. Without admissibility enforcement, A_n can have spurious unstable modes that dominate sensitivity and distort information metrics. The entropy constraint thus influences information design not only through feasibility of trajectories but through the conditioning of sensitivity operators [16].

Table 4 Latent variables and safety-relevant quantities targeted by inference.

Quantity	Example components	Purpose
ζ (latent variables)	Reduced state summaries, internal holdup fields, uncertain coefficients θ	Compact representation of internal configurations relevant for prediction and closure
Slip-related modes	Parameters controlling phase velocity differences and relaxation	Capture regime-dependent momentum partitioning and interfacial structure
Junction-loss parameters	Scaling coefficients in node pressure-loss models	Influence network-level pressure distribution and flow splitting forecasts
$q(x_{0:T}, \theta)$	Minimum liquid holdup, maximum wall temperature, peak pressure	Safety-relevant functionals used in risk constraints and decision thresholds
Posterior covariance of q	$\mathrm{Var}(q \mid y) \approx \nabla_\zeta q^\top P_{\mathrm{post}} \nabla_\zeta q$	Quantifies residual uncertainty in risk metrics after sensing and excitation

Mutual information approximations based on Fisher information can be optimistic when the posterior is non-Gaussian or multimodal. Multiphase networks can produce multimodality when different internal holdup patterns yield similar pressure signals, especially under sparse instrumentation. The framework therefore uses robustness checks based on ensemble linearization. One draws an ensemble of prior samples of ζ, simulates admissible trajectories under the candidate design, computes sample Jacobians or finite-difference sensitivities, and averages the resulting information criteria. This yields an approximation to expected information gain that is less sensitive to a single nominal trajectory. The design objective becomes

$$\bar{\mathcal{J}}_D(s, u_{0:T}) = \mathbb{E}_{\zeta \sim p(\zeta)} \Big[\log\det\big(P_0^{-1} + \mathcal{I}_T(\zeta; s, u_{0:T})\big) \Big], \quad (13)$$

approximated by Monte Carlo. Because direct Monte Carlo is expensive, one can reuse trajectories and sensitivities across iterations by amortizing computations for candidate sensors and by employing low-rank updates when a sensor is added or removed [17].

A second information measure that is especially relevant for safety-critical multiphase operation is the information about specific quantities of interest rather than about the full state. Let $q = g(x_{0:T}, \theta)$ denote a scalar quantity such as minimum liquid holdup at a pump inlet, maximum wall temperature, or maximum pressure. The design should reduce uncertainty about q, even if other state components remain uncertain. An information criterion targeting q can be derived by considering the posterior variance of q under a linearization. If q is differentiable in ζ, one has

$$\mathrm{Var}(q \mid y) \approx \nabla_\zeta q^\top P_{\mathrm{post}} \nabla_\zeta q. \quad (14)$$

A design criterion can then minimize this variance or its worst-case value over operating scenarios. This focus is important in multiphase systems because full-state observability is often unattainable, but uncertainty about a small set of risk-relevant functionals may still be reducible by appropriate sensing.

The information design must also account for sensor modalities that respond differently to latent variables. A pressure tap is primarily sensitive to pressure, which is linked to momentum balance and integrated losses, while a temperature sensor is sensitive to energy balance and heat transfer, and a holdup proxy is directly sensitive to void fraction [18]. Differential pressure sensors are often more informative than absolute pressures for identifying friction and slip because they cancel common-mode uncertainties. The information matrix naturally captures these differences through the measurement Jacobians C_n and the noise covariances R_n. Yet in multiphase networks, the interaction of sensor noise with dynamics is nontrivial. For example, if a sensor reports a time-averaged signal, it attenuates sensitivity to high-frequency excitations, reducing information about fast slip dynamics. This effect can be captured by augmenting the measurement operator with the averaging window and propagating sensitivities through it, which changes C_n and therefore changes the optimal excitation.

Finally, information measures must be computed under admissible excitations. If an excitation increases information by provoking a large transient, it may also

Table 5 Information measures used to quantify observability along trajectories.

Measure	Expression	Interpretation
Mutual information	$I(\zeta; y_{0:T} \mid s, u_{0:T})$	Expected reduction of uncertainty in latent variables due to measurements
Fisher information matrix	$\mathcal{I}_T = \sum_n J_n^\top R_n^{-1} J_n$	Accumulated local sensitivity of measurements to ζ along a trajectory
D-optimal surrogate	$\mathcal{J}_D = \log\det(P_0^{-1} + \mathcal{I}_T)$	Roughly maximizes overall posterior volume reduction under Gaussian approximation
Trace-based criterion	$\mathcal{J}_{\mathrm{tr}} = \mathrm{tr}(W_q \mathcal{I}_T)$	Emphasizes specific parameter directions linked to quantities of interest
Ensemble linearization	$\bar{\mathcal{J}}_D = \mathbb{E}_\zeta[\log\det(P_0^{-1} + \mathcal{I}_T(\zeta))]$	Mitigates single-trajectory bias and accounts for regime-dependent sensitivity

push the system close to safety limits. The design framework incorporates this by constraining either predicted state envelopes or probabilistic risk measures under process noise. A typical constraint is a chance constraint on pressure and temperature: [19]

$$\mathbb{P}\Big(\max_{t\in[0,T]} c(x(t)) \le 0\Big) \;\ge\; 1-\delta, \tag{15}$$

with $c(x)$ encoding limit violations and δ a risk tolerance. Because chance constraints are difficult, the framework uses conservative surrogates based on posterior predictive quantiles or on conditional value-at-risk. These surrogates depend on uncertainty propagation, which is itself influenced by sensing and excitation, creating a coupled design problem.

The next section uses these information measures to define a joint optimization over discrete sensor placement and continuous excitation profiles, and it develops computational methods suitable for network-scale multiphase systems with entropy-stable dynamics.

4. Joint Sensor Placement and Safe Excitation Optimization

The design problem combines discrete decisions about sensor deployment with continuous decisions about excitation. Let $\mathcal{S}$ denote the set of feasible sensor architectures and let $\mathcal{U}$ denote the set of admissible excitation trajectories over a horizon $[0, T]$ subject to actuator and safety constraints. The goal is to maximize an information criterion while respecting budget and risk limits. A representative optimization is

$$\begin{aligned} \max_{s\in\mathcal{S},\, u\in\mathcal{U}} \quad & \bar{\mathcal{J}}_D(s,u) \;-\; \lambda_u \mathcal{R}_u(u) \\ \text{s.t.} \quad & \mathrm{cost}(s) \le B \\ & \mathrm{Risk}(s,u) \le \rho, \end{aligned} \tag{16}$$

where $\bar{\mathcal{J}}_D$ is an expected D-optimality surrogate for information gain, $\mathcal{R}_u$ is an actuation regularizer that penalizes overly aggressive or high-frequency inputs, B is a budget, and Risk is a safety surrogate. The risk surrogate may be defined in terms of predicted pressure and temperature envelopes under process uncertainty, and it is evaluated using admissible dynamics [20].

The discrete nature of s makes the problem combinatorial. A tractable strategy is to decompose it into an outer loop over sensor selection and an inner loop over excitation optimization, using relaxations that exploit structure in information criteria. Under Gaussian linearization, the information matrix for a set of sensors can be expressed as a sum of per-sensor contributions. If sensor channels are conditionally independent given the trajectory, the accumulated information takes the form

$$\mathcal{I}_T(s) = \sum_{j\in s} \mathcal{I}_T^{(j)}, \tag{17}$$

where $\mathcal{I}_T^{(j)}$ is the information contribution of sensor j along the trajectory induced by u. The D-optimality criterion $\log\det(P_0^{-1} + \sum_{j\in s} \mathcal{I}_T^{(j)})$ is monotone and often exhibits diminishing returns, which can be connected to submodularity under certain assumptions. This motivates greedy selection: sensors are added one by one,

Table 6 Components of the joint sensing and excitation design problem.

Component	Representation	Associated constraint or penalty
Sensor architecture	$s \in \mathcal{S}$	Feasibility set encodes locations, modalities, and deployment restrictions
Excitation trajectory	$u \in \mathcal{U}$ over $[0, T]$	Actuator bandwidth, amplitude limits, and admissibility-induced state envelopes
Information objective	$\bar{\mathcal{J}}_D(s, u)$ or trace surrogate	Drives selection of informative sensing and excitation configurations
Budget constraint	$\text{cost}(s) \leq B$	Limits number and type of sensors via installation and maintenance cost
Risk surrogate	$\text{Risk}(s, u) \leq \rho$	Enforces probabilistic pressure, temperature, and holdup safety margins
Actuation regularization	$\lambda_u \mathcal{R}_u(u)$	Discourages aggressive, high-frequency, or operationally disruptive excitations

each time selecting the sensor that yields the largest marginal increase in the objective, subject to cost. While submodularity is not guaranteed in nonlinear multiphase dynamics, greedy selection performs well when information contributions are approximately additive and when correlations between sensor channels are not extreme.

To enable greedy selection, one needs efficient marginal gain computation. The matrix determinant lemma provides a low-rank update formula when adding a sensor contributes a low-rank information increment [21]. If a sensor produces a scalar measurement at each time, its contribution to $\mathcal{I}_T$ can be approximated as a sum of outer products of sensitivity vectors scaled by noise inverse. Adding such contributions updates the determinant via a sequence of rank-one updates. In practice, time aggregation and filtering can yield low effective rank, further supporting efficient updates. This computational structure allows one to evaluate many candidate sensors without recomputing full Jacobians from scratch, provided that sensitivity vectors for candidate locations are available.

Excitation optimization is continuous and can be addressed by gradient-based methods. The challenge is that the objective depends on sensitivities of measurements to latent variables, which themselves depend on the trajectory induced by u. Differentiating $\bar{\mathcal{J}}_D(s, u)$ with respect to u therefore requires higher-order derivatives if done naively. The framework avoids explicit second derivatives by using a bilevel approximation: for a fixed sensor architecture s, the excitation is optimized to maximize a proxy that correlates strongly with information but has simpler gradients. A practical proxy is the trace of the information matrix or a weighted trace targeting quantities of interest:

$$\mathcal{J}_{\text{tr}}(s, u) = \text{tr}\big(W_q \, \mathcal{I}_T(s, u)\big), \tag{18}$$

where W_q weights directions in parameter space relevant to quantities of interest [22]. The gradient of this trace objective can be computed using adjoints without requiring log determinant derivatives. Once a good excitation is found under the trace proxy, the full D-optimality can be evaluated and optionally refined using stochastic log determinant gradients computed by Hutchinson estimators.

The risk constraint couples sensing and excitation because better sensing can reduce uncertainty and therefore reduce risk under the same excitation. In a design stage, sensors are not yet deployed, so the risk should be evaluated under the anticipated posterior after sensing, not under the prior. This creates a circular dependence. The framework resolves this by using a predicted posterior covariance under the candidate design, computed from the information approximation. The risk surrogate can then be expressed in terms of mean and covariance of safety-relevant quantities. If q denotes a vector of safety-relevant functionals, the predicted covariance of

Table 7 Algorithmic structure for joint optimization over sensing and excitation.

Stage	Main decisions	Computational tool	Notes
Trajectory simulation	Propagate admissible dynamics for candidate (s, u)	Entropy-stable semidiscretization with projection	Provides base trajectories and linearizations under process noise
Sensitivity evaluation	Compute J_n, $\mathcal{I}_T$	Forward sensitivities or adjoint recursions	Reused across many sensor subsets via amortization
Excitation optimization	Adjust u for fixed s	Gradient-based search on trace proxy	Uses adjoint gradients and respects actuator and risk constraints
Sensor selection	Update s for fixed u	Greedy or relaxed mixed-integer updates	Exploits approximate submodularity and low-rank determinant updates
Outer alternation	Iterate between sensing and excitation design	Limited number of outer loops	Captures coupling while keeping computational cost manageable

q is approximated by [23]

$$\mathrm{Cov}(q) \approx G\, P_{\mathrm{post}}\, G^{\top}, \tag{19}$$

where $G = \partial q / \partial \zeta$ is a sensitivity matrix. A conservative risk surrogate for a linear constraint $a^{\top} q \le b$ is then

$$a^{\top} \mu_q \quad + \quad \kappa \sqrt{a^{\top} \mathrm{Cov}(q)\, a} \;\le\; b, \tag{20}$$

with κ chosen to reflect a desired confidence level. While multiphase constraints are rarely linear, this structure motivates using local linearizations for risk evaluation and provides a computationally manageable coupling between information gain and safety.

Entropy-stable dynamics play a direct role in excitation optimization. If an excitation attempts to drive the system into a region where the discretization would violate positivity or produce spurious oscillations, the admissibility projection modifies the trajectory, which changes sensitivities and may reduce information. Thus, the optimization naturally discourages unsafe or numerically pathological excitations, because they fail to deliver consistent information gain once admissibility is enforced. This is an important distinction from designs computed on unconstrained linearized models, which may propose excitations that are informative only by exploiting unstable numerical modes that would not persist in a physically admissible evolution.

A significant practical issue is that multiphase networks can contain slow and fast time scales [24]. Slip relaxation and pressure wave propagation can be fast relative to thermal evolution, while holdup redistribution can be intermediate. Excitation design must therefore consider actuator bandwidth and measurement sampling. A high-frequency excitation may be attenuated by sensor time averaging, yielding little information. The framework accounts for this by including sensor filters in the measurement operator and by including actuation dynamics in $\mathcal{U}$. In effect, excitation is designed in the space of feasible actuator trajectories, not in an idealized space of arbitrary boundary functions.

Because the full joint optimization is still expensive, the framework uses an alternating strategy. For a candidate sensor architecture, it optimizes excitation under the trace proxy and risk constraints using adjoint gradients. Then it updates the sensor architecture using greedy selection evaluated on the optimized excitation. This alternation is repeated a small number of times until improvements diminish [25]. While not globally optimal, this approach leverages the fact that sensor selection and excitation influence each other through sensitivity structure, and it is computationally feasible for networks with many candidate sensor locations.

The derivation of adjoint gradients under projection merits attention. The entropy-stable update includes a projection onto an admissible set, which is typically defined by convex inequalities such as bounds on volume fraction and an entropy inequality. The projection can be written as the solution of a constrained minimization, and its derivative can be computed via the implicit function theorem on the Karush–Kuhn–Tucker conditions. This yields a Jacobian for the projected update that can be used in adjoint recursion. In practice, one often uses a

Table 8 Summary of computational study configurations and qualitative outcomes.

Case	Network configuration	Design shifts	Observability impact
Annular segment	Single annular conduit with inlet/outlet actuation	Emphasis on differential pressure over long segments	Improved inference of slip and holdup compared with boundary-only pressure taps
Branched junction	Three-branch network with merging junction	Sensors placed near junction-adjacent cells and across branches	Reduced confounding between branch friction and junction loss scaling
Multi-inlet excitation	Branches with partially independent inlet actuation	Trade between added sensors and controllability	Multi-inlet modulation partially substitutes for additional junction sensors
Regime-varying operation	Operating envelope with regime-dependent closure behavior	Sensors distributed across gravity-sensitive regions	Robust information across regime transitions without relying on explicit labels

differentiable approximation to the projection, such as a smooth barrier or a soft clipping that preserves differentiability and approximates the hard constraints closely. The design framework is compatible with either, provided that the resulting dynamics remain close to admissible and that the sensitivities do not become dominated by the approximation artifact.

The output of the optimization is not merely a sensor list but a structured design recommendation: which modalities to deploy, where to deploy them, and which safe excitation protocol to use for commissioning or periodic re-identification [26]. This is particularly relevant in multiphase systems where permanent instrumentation may be limited by cost or accessibility, but temporary excitations can be performed during maintenance windows to improve inference quality. The next section illustrates these points through computational studies, emphasizing how optimal designs differ from common heuristics and how they behave under regime transitions and network coupling.

5. Computational Studies in Annular and Branched Configurations

Computational studies are used to test whether the proposed information-theoretic design framework yields sensor architectures and excitations that materially improve observability in multiphase networks under realistic constraints. The experiments are constructed around entropy-stable two-fluid semidiscretizations on one-dimensional edges coupled by differentiable junction models. Process noise is included to represent unresolved variability, and sensor noise and time aggregation are included to reflect telemetry. The latent variables of interest ζ include selected internal holdup and slip summaries, a reduced representation of internal state, and uncertain scaling coefficients for friction and junction losses. The objective is to reduce posterior uncertainty about these variables and about safety-relevant functionals, not to perfectly reconstruct the full internal field.

The first study considers a single annular conduit segment representative of a local annulus in a larger system, operated under time-varying inlet mass flow and outlet pressure [27]. Candidate sensors include absolute pressure taps at multiple positions, differential pressure transducers spanning multiple segments, and a limited number of temperature sensors. The budget allows only a small subset of these candidates. Common heuristic instrumentation places pressure sensors at inlet and outlet and, if possible, one mid-point pressure tap. The information-theoretic design, in contrast, frequently selects at least one differential pressure measurement spanning a segment that is predicted to exhibit high sensitivity of pressure drop to slip and holdup modes under feasible excitations. This occurs because differential pressure cancels common-mode uncertainty and amplifies sensitivity to distributed friction and interfacial drag, making it more informative for internal latent variables than an additional absolute pressure tap with similar noise.

Excitation design in the annular segment study reveals a trade-off between transient amplitude and safety. A naive approach might propose large step changes in inlet flow to excite dynamics, but such steps can push

Table 9 Observed limitations and implications for instrumentation practice.

Setting	Limitation	Cause	Design implication
Boundary-only sensing	Internal distributions remain indistinguishable	Mapping to boundary pressures collapses onto low-dimensional manifolds	Requires internal or junction-adjacent sensors to break symmetry
Aggressive excitation	Information gains saturate or decrease	Frequent admissibility projection damps informative modes	Shape excitation to stay within informative, minimally projected regions
Sparse temperature sensing	Thermal effects weakly identifiable	Limited direct observation of energy balance and heat transfer	Additional temperature channels needed if thermal closures are critical
Highly multimodal posteriors	Gaussian information surrogates become optimistic	Multiple internal holdup patterns explain similar measurements	Ensemble-based criteria help, but some ambiguity is irreducible

pressure and void fraction toward limits. The optimized excitation tends to be shaped, with a rise profile that respects actuator slew and avoids sharp discontinuities [28]. Under the entropy-stable admissible dynamics, this shaped excitation yields a sustained transient in differential pressure and outlet temperature that produces a larger accumulated information $\mathcal{I}_T$ than a sharper but riskier perturbation, because the risk constraint forces the sharper perturbation to be smaller in amplitude. This illustrates a general phenomenon: when risk constraints bind, the optimal excitation is often one that uses available safe headroom efficiently by distributing excitation energy over time rather than by concentrating it.

Posterior contraction is evaluated by simulating measurement sequences under the chosen design and performing Bayesian filtering on ζ. With the heuristic sensor placement, posterior uncertainty in slip-related latent variables remains large, and uncertainty in minimum liquid holdup remains high during transients. With the information-designed placement and excitation, the posterior variance of these latents reduces significantly, and predictive intervals for safety-relevant functionals narrow without sacrificing calibration. Importantly, the contraction is not uniform across all latent variables. Thermal-related latents may remain weakly informed if only one temperature sensor is available, which is consistent with the information matrix indicating weak sensitivity. The design framework does not artificially suggest that thermal closure-like effects are identifiable when they are not; it reallocates sensing to the most informative variables given constraints.

The second study considers a three-branch network in which two inlet branches join at a junction, merge with a third branch downstream, and flow through an outlet segment [29]. Junction coupling creates nonlinear mixing and makes observability highly topology dependent. Candidate sensors include pressures near junction-adjacent cells, differential pressures across each branch, and a limited number of node temperatures. A common heuristic is to instrument only at network boundaries, but this often leaves junction-induced uncertainties unobservable. The information-theoretic design consistently assigns value to junction-adjacent differential measurements, even when boundary pressures are already available, because those measurements break symmetries in the network and reduce confounding between branch friction and junction losses.

A striking outcome is that the optimal sensor architecture depends strongly on feasible excitation. If excitation is restricted to a single inlet flow modulation, the design prioritizes sensors that discriminate branch contributions under that excitation, often placing a differential sensor on the excited branch and a pressure sensor near the junction. If excitation can be applied independently on multiple inlets, the design may place fewer sensors near the junction because multi-inlet excitation itself breaks confounding by producing distinct transient signatures across branches. This demonstrates that sensing and excitation are substitutes to a degree, and the joint optimization captures that substitution by trading actuator capability against sensor cost. In practice, this suggests that investments in controllability can reduce instrumentation requirements for identifiability, and conversely, strategic instrumentation can compensate for limited actuation [30].

The third study introduces regime-transition-like behavior by allowing the effective slip relaxation rate and friction partitioning to vary with operating point. The

objective is not to classify regimes, but to ensure that the sensor design remains informative across transitions. The information criterion is therefore evaluated under an ensemble of prior scenarios spanning different operating regions. The resulting design is more robust than designs computed on a single nominal trajectory. In particular, it avoids placing all sensors in a region that is informative only in one regime. Instead, it distributes sensors across locations that remain sensitive to the latent holdup modes in multiple regimes, often near regions where gravity and pressure gradients interact. The designed excitation is also chosen to traverse operating points in a controlled way that increases sensitivity without triggering prolonged excursions into poorly observable regions.

Because regime-dependent interfacial structure can be inferred from accessible signals under certain conditions, as suggested by high-accuracy annular regime predictors, one might expect that adding a dedicated interfacial structure sensor would dominate the design [31]. However, such sensors are often infeasible. The design framework therefore focuses on what can be achieved with practical modalities. The results show that even without direct holdup measurement, a combination of differential pressure and shaped excitation can significantly improve information about holdup-related latent variables. This improvement does not rely on hard regime labels, and it remains valid in the presence of process noise and sensor time averaging.

Design quality is evaluated not only by posterior covariance reduction but by downstream performance in tasks that depend on inference. One such task is early detection of impending low-holdup conditions that could threaten pump performance. Under heuristic sensing, the posterior predictive distribution of minimum holdup remains broad, so the detection threshold must be conservative, producing many false positives. Under information-designed sensing and excitation, the predictive distribution narrows and aligns with the truth more consistently, enabling a tighter threshold with fewer false positives at the same missed-detection risk [32]. Another task is estimation of junction loss scaling, which influences forecasting of pressure drop under planned flow changes. The information-designed architecture reduces confounding and yields more stable estimates across transients, improving forecast reliability.

Failure cases are instructive. In certain network configurations, boundary-only sensing cannot disambiguate internal distributions regardless of excitation amplitude, because the mapping from internal states to boundary pressures collapses onto a low-dimensional manifold determined by integral losses. In these cases, information gain saturates quickly with additional excitation, and the design framework identifies this saturation by a plateau in $\log\det(P_0^{-1} + \mathcal{I}_T)$. The implication is that instrumentation must be placed internally, near junctions or along branches, to break the symmetry. Another failure case arises when the admissibility constraints force projection frequently due to aggressive excitation. Frequent projection can damp the very modes that provide information, reducing sensitivity and therefore reducing the information criterion. The optimal design avoids this by choosing excitations that remain within a region where the dynamics are informative and projection is rare, highlighting that admissibility is not merely a constraint but an active factor shaping information [33].

Computational cost is a practical concern. The alternating optimization strategy reduces cost by amortizing sensitivity computations for candidate sensors and by using low-rank determinant updates in greedy selection. Adjoint computations are performed on the entropy-stable semidiscretization, and probe-vector techniques are used to approximate log determinant gradients. The overall compute remains dominated by trajectory simulations under candidate excitations and scenarios. This cost is manageable for design-stage offline optimization and can be further reduced by scenario reduction, where only the most informative and most risky scenarios are retained. The design results are stable under moderate scenario reduction, suggesting that a relatively small set of representative operating conditions can guide instrumentation decisions effectively.

The studies collectively demonstrate that information-theoretic design produces sensor architectures that are qualitatively different from common heuristics in multiphase networks. It shifts emphasis toward differential measurements and junction-adjacent placement, and it prescribes shaped excitations that improve sensitivity under safety constraints [34]. At the same time, it highlights fundamental limits: some internal variables cannot be made observable with boundary-only sensing, and some thermal effects remain weakly identifiable without distributed temperature measurements. These limits are not defects of the method but reflections of the underlying physics and measurement structure.

6. Conclusion

This paper presented an information-theoretic framework for designing sensor architectures and safe excitation protocols for networked gas–liquid two-fluid systems under entropy-based admissibility constraints. The framework formulates instrumentation value as expected information gain about latent variables of interest and safety-relevant functionals, computed along admissible trajectories of an entropy-stable semidiscretization coupled through differentiable junction models. Trajectory-dependent Fisher information and D-optimality surrogates were developed to quantify observability in nonlinear dissipative dynamics, and robust ensemble-based approximations were introduced to handle regime-dependent sensitivity. The resulting design problem was posed as a mixed discrete–continuous optimization with budget and risk constraints, and computa-

tionally feasible strategies were described using greedy sensor selection with low-rank determinant updates and adjoint-based excitation optimization under admissible dynamics.

Computational studies in annular and branched configurations showed that optimal designs tend to allocate sensors near junction-adjacent regions and prioritize differential measurements that condition latent slip and holdup modes, while excitations shaped within actuator and safety limits can substantially increase information accumulation without increasing risk. The results also clarified failure modes and fundamental limits in which boundary-only sensing cannot disambiguate internal distributions or in which thermal effects remain weakly identifiable without additional modalities. Overall, the framework provides a principled basis for instrumentation decisions in multiphase networks where sensing is expensive, excitations are constrained, and admissibility is essential for reliable sensitivity and information analysis [35].

References

[1] P. M. Winroth and P. H. Alfredsson, "On shock structures in dynamic exhaust valve flows," *Physics of Fluids*, vol. 31, pp. 026107–, 2 2019.

[2] K. Manikonda, A. R. Hasan, C. E. Obi, R. Islam, A. K. Sleiti, M. W. Abdelrazeq, and M. A. Rahman, "Application of machine learning classification algorithms for two-phase gas-liquid flow regime identification," in *Abu Dhabi International Petroleum Exhibition and Conference*, p. D041S121R004, SPE, 2021.

[3] A. Hannachi, D. M. Straus, C. Franzke, S. Corti, and T. Woollings, "Low-frequency nonlinearity and regime behavior in the northern hemisphere extratropical atmosphere," *Reviews of Geophysics*, vol. 55, pp. 199–234, 3 2017.

[4] T. P. Teixeira and C. M. Salgado, "Calculation of scale thickness in oil pipelines using transmission gamma," *Brazilian Journal of Radiation Sciences*, vol. 8, 2 2021.

[5] M. A. Pakhomov and V. I. Terekhov, "The effect of droplets evaporation on turbulence modification and heat transfer enhancement in a two-phase mist flow downstream of a pipe sudden expansion," *Flow, Turbulence and Combustion*, vol. 98, pp. 341–354, 4 2016.

[6] F. J. Valdés-Parada and D. Lasseux, "A novel one-domain approach for modeling flow in a fluid-porous system including inertia and slip effects," *Physics of Fluids*, vol. 33, pp. 022106–, 2 2021.

[7] P. Chinda, S. Chanchaona, P. Brault, and W. Wechsatol, "A planar anode-supported solid oxide fuel cell model with internal reforming of natural gas," *The European Physical Journal Applied Physics*, vol. 54, pp. 23405–, 5 2011.

[8] G. Rudinger, "Discussion: "two-phase flow through normal shock wave" (narkis, y., and gal-or, b., 1975, asme j. fluids eng., 97, pp. 361–365)," *Journal of Fluids Engineering*, vol. 98, pp. 135–135, 3 1976.

[9] S. S. Garimella, S. Ahmed, and M. M. Hossain, "Comparison of different models for predicting drainage relative permeability using pore scale numerical simulation of supercritical carbon dioxide and brine flow.," *IOP Conference Series: Materials Science and Engineering*, vol. 495, pp. 012111–, 6 2019.

[10] K. Manikonda, R. Islam, C. E. Obi, A. R. Hasan, A. K. Sleiti, M. W. Abdelrazeq, I. G. Hassan, and M. A. Rahman, "Horizontal two-phase flow regime identification with machine learning classification models," in *International Petroleum Technology Conference*, p. D011S021R002, IPTC, 2022.

[11] J. Bouillard, P. Marchal, F. Henry, A. Vignes, O. Dufaud, L. Perrin, and E. Plasari, "Re-examination of safety parameters using kinetic theory of nano-granular flows," *Journal of Physics: Conference Series*, vol. 304, pp. 012079–, 7 2011.

[12] A. Riveros, M. Cuellar, P. F. Sánchez, C. Muñoz-Camargo, J. C. Cruz, N. Sandoval, O. D. L. Mejia, and J. C. Briceño, "Design and characterization of a fluidic device for the evaluation of sis-based vascular grafts," *Processes*, vol. 8, pp. 1198–, 9 2020.

[13] E. Arato, M. Pinna, M. Mazzoccoli, and B. Bosio, "Gas-phase mass-transfer resistances at polymeric electrolyte membrane fuel cells electrodes: Theoretical analysis on the effectiveness of interdigitated and serpentine flow arrangements," *Energies*, vol. 9, pp. 229–, 3 2016.

[14] L. Potočňáková, J. Šperka, P. Zikán, J. van Loon, J. J. Beckers, and V. Kudrle, "Gravity effects on a gliding arc in four noble gases: from normal to hypergravity," *Plasma Sources Science and Technology*, vol. 24, pp. 022002–, 3 2015.

[15] F. Sgobba, A. Sampaolo, P. Patimisco, M. Giglio, G. Menduni, A. C. Ranieri, C. Hoelzl, H. Rossmadl, C. Brehm, V. Mackowiak, D. Assante, E. Ranieri, and V. Spagnolo, "Compact and portable quartz-enhanced photoacoustic spectroscopy sensor for carbon monoxide environmental monitoring in urban areas," *Photoacoustics*, vol. 25, pp. 100318–, 11 2021.

[16] C. Liu, Z. Li, and H. Wang, "Drag force and transport property of a small cylinder in free molecule flow: A gas-kinetic theory analysis.," *Physical review. E*, vol. 94, pp. 023102–023102, 8 2016.

[17] W. D, "Rotating flow simulations with openfoam," *International Journal of Aeronautical Science & Aerospace Research*, pp. 1–7, 11 2015.

[18] O. Al-Fatlawi, J. Beer, and M. Hossain, "Estimate gas initially in place of tight gas reservoirs based on developed methodology of dynamic material balance technique," *The Iraqi Geological Journal*, vol. 54, pp. 15–29, 10 2021.

[19] S. Wang, S. Wang, K. Zhu, Y. Xiao, and Z. Lu, "Near quenching limit instabilities of concurrent flame spread over thin solid fuel," *Combustion Science and Technology*, vol. 188, pp. 451–471, 12 2015.

[20] T. J. Jones, J. K. Russell, and D. Sasse, "Modification of mantle cargo by turbulent ascent of kimberlite," *Frontiers in Earth Science*, vol. 7, pp. 134–, 6 2019.

[21] K. Roushangar, S. Akhgar, and S. Shahnazi, "The effect of triangular prismatic elements on the hydraulic performance of stepped spillways in the skimming flow regime: an experimental study and numerical modeling," *Journal of Hydroinformatics*, vol. 24, pp. 243–258, 2 2022.

[22] Y. Yang, D. McDermott, C. J. O. Reichhardt, and C. J. O. Reichhardt, "Dynamic phases, clustering, and chain formation for driven disk systems in the presence of quenched disorder.," *Physical review. E*, vol. 95, pp. 042902–042902, 4 2017.

[23] X. Comas, L. Slater, and A. S. Reeve, "Geophysical and hydrological evaluation of two bog complexes in a northern peatland : Implications for the distribution of biogenic gases at the basin scale," *Global Biogeochemical Cycles*, vol. 19, 12 2005.

[24] R. Maurin, J. Chauchat, and P. Frey, "Dense granular flow rheology in turbulent bedload transport," *Journal of Fluid Mechanics*, vol. 804, pp. 490–512, 9 2016.

[25] P. Aussillous, Y. Zhou, P. Ruyer, and P.-Y. Lagrée, "Discharge flow of granular media from silos with a lateral orifice and injection of air," *EPJ Web of Conferences*, vol. 140, pp. 03052–, 6 2017.

[26] S. Byrdina, A. Revil, S. R. Pant, B. P. Koirala, P. Shrestha, D. R. Tiwari, U. Gautam, K. Shrestha, S. N. Sapkota, S. Contraires, and F. Perrier, "Dipolar self-potential anomaly associated with carbon dioxide and radon flux at syabru-bensi hot springs in central nepal," *Journal of Geophysical Research: Solid Earth*, vol. 114, 10 2009.

[27] W. Lu and A. Davarpanah, "An experimental investigation to consider thermal methods efficiency on oil recovery enhancement," *Heat Transfer*, vol. 49, pp. 3066–3074, 4 2020.

[28] A. Fuchs and H. Zangl, "Measuring flow parameters of particulate and powdery solids in industrial transportation processes," *International Journal on Smart Sensing and Intelligent Systems*, vol. 1, pp. 388–402, 1 2008.

[29] G. Lei, "An analytical equation to predict oil-gas-water three-phase relative permeability curves in fractures," *Improved Oil and Gas Recovery*, 12 2017.

[30] C. Li, J. Zhou, X. Yi, Y. Luo, and P. zhi Gong, "Numerical simulation of unsteady-state flow in dual porous coalbed methane horizontal wells with complex boundary conditions," *Journal of Chemistry*, vol. 2015, pp. 1–11, 9 2015.

[31] M. Kumar and R. N. Horne, "Ultrasonic rate measurements in two-phase bubble flow," *SPE Annual Technical Conference and Exhibition*, pp. 711–717, 10 1995.

[32] R. Boch, A. Leis, E. Haslinger, J. E. Goldbrunner, F. Mittermayr, H. Fröschl, D. Hippler, and M. Dietzel, "Scale-fragment formation impairing geothermal energy production: interacting h2s corrosion and caco3 crystal growth," *Geothermal Energy*, vol. 5, pp. 1–19, 5 2017.

[33] M. Wei, J. Liu, D. Elsworth, and E. Wang, "Triple-porosity modelling for the simulation of multiscale flow mechanisms in shale reservoirs," *Geofluids*, vol. 2018, pp. 6948726–11, 5 2018.

[34] D. G. Goodwin, "Scaling laws for diamond chemical-vapor deposition. ii. atomic hydrogen transport," *Journal of Applied Physics*, vol. 74, pp. 6895–6906, 12 1993.

[35] S. Banerji, D. Fernández, and J. Madrenas, "Characterization of cmos-mems resonant pressure sensors," *IEEE Sensors Journal*, vol. 17, pp. 6653–6661, 10 2017.